

# Understanding Microscopic Properties of Light-Emitting Diodes from Macroscopic Characterization: Ideality Factor, S-parameter, and Internal Quantum Efficiency

Dong-Soo Shin and Jong-In Shim\*

Herein, how the macroscopic characterizations can be utilized to extract information on the defect level and crystal quality of the epitaxial layers of the light-emitting diodes (LEDs) is presented. After review of the current–voltage ( $I$ – $V$ ) and light output power–current ( $L$ – $I$ ) characteristics, actual examples are utilized to show how different defect levels in the devices are reflected in macroscopic characteristics including the internal quantum efficiency (IQE). We show that the ideality factor from the  $I$ – $V$  and the S-parameter from the  $L$ – $I$  can serve as useful guides to denote the dominance of the radiative recombination in the active region of the device. The minimum ideality factor is proposed as a possible figure of merit for the defect level of the epitaxial layers of the device and shown to be correlated with the maximum IQE value.

## 1. Introduction

Microscopic properties of semiconductors affect the performance of optoelectronic devices in fundamental ways. In light-emitting diodes (LEDs), microscopic crystalline defects act as nonradiative recombination centers and tend to induce nonradiative recombinations, reducing the internal quantum efficiency (IQE) of the device.<sup>[1–3]</sup> The level of defects in semiconductors also limits the reliability of the optoelectronic devices as the prolonged operation generates defects and subsequently deteriorates the device performance.<sup>[4,5]</sup> In this sense, the information on the defect level in optoelectronic devices is considered critically important.

Numerous researches have been performed to investigate the microscopic properties of semiconductors, especially various crystalline defects, with microscopic tools such as scanning or transmission electron microscopy, near-field optical microscopy, and scanning-capacitance microscopy.<sup>[3,6–10]</sup> However, the aspect of how the level of microscopic defects influence the device characteristics such as current–voltage ( $I$ – $V$ ) and light output power–current ( $L$ – $I$ ) have so far been examined rather insufficiently and

systematic understanding of how one can extract the information on the level of defects from the device characteristics needs more attention.

In this article, using InGaN-based blue LEDs, we summarize how the optoelectronic performance of the device is affected by defects and demonstrate how the information on the defect level in the device can be extracted systematically from the macroscopic characterizations. These understandings can be very useful in comparing devices from different epitaxial layers or fabrication processes and also in finding a useful measure of defect level in the device. We review especially the ideality factor, the S-parameter, and the IQE of

the LED device and examine the interrelations between these parameters. As the device size becomes ever smaller for applications in displays, considerations given in this article can be a very useful guide for further characterizing the micro-sized LEDs.

## 2. Optoelectronic Performance Characterization

### 2.1. $I$ – $V$ Characteristics and the Ideality Factor

The  $I$ – $V$  curve is frequently measured to check the electrical characteristics of a device. One can obtain information on an appropriate forward voltage for the given forward current to generate a certain amount of optical power in the case of LEDs. The voltage that needs to be applied typically increases with the bandgap energy of the materials that the LED is made of. The  $I$ – $V$  characteristics are often represented by the Shockley equation


$$I \cong I_s e^{qV_j/kT} \sim e^{(qV_j - E_g)/kT} \quad (1)$$

where the device injection current  $I$  is expressed in terms of the reverse saturation current  $I_s$ , the elementary charge  $q$ , the junction voltage  $V_j$ , the Boltzmann constant  $k$ , the absolute temperature  $T$ , and the bandgap energy  $E_g$ . The junction voltage  $V_j$  differs from the externally applied voltage  $V$  by the voltage drop outside the active region caused by the series resistance  $R_s$ , i.e.

$$V_j = V - IR_s \quad (2)$$

Since  $I_s$  depends on  $E_g$  in the functional form  $I_s \sim \exp(-E_g/kT)$ ,<sup>[11]</sup>  $V_j$  greater than  $E_g/q$  should be applied to turn on the diode as represented in Equation (1), which is

D.-S. Shin, J.-I. Shim  
 Department of Photonics and Nanoelectronics and BK21 FOUR ERICA-ACE Center  
 Hanyang University ERICA  
 Ansan, Gyeonggi-do 15588, Korea  
 E-mail: jishim@hanyang.ac.kr

 The ORCID identification number(s) for the author(s) of this article can be found under <https://doi.org/10.1002/pssa.202200042>.

DOI: 10.1002/pssa.202200042

the reason behind the dependence of the forward voltage on the bandgap energy of the material.

**Figure 1** shows an example of how the device turn-on depends on the bandgap energy of the material that the LED is made of, exhibiting the importance of the bandgap energy as described in Equation (1). It is seen that the infrared LED with a peak wavelength  $\lambda_p = 860$  nm (1.44 eV) turns on at approximately 1.2 V while the blue LED with a peak wavelength  $\lambda_p = 450$  nm (2.75 eV) turns on at approximately 2.6 V.

While the current after turn-on can be described by the Shockley equation with the series resistance into account, more information can be obtained from the low-current range near turn-on. For this purpose, the  $I$ - $V$  characteristics are typically checked with the semi-log plots, where the current is expressed on log scales. As known from the recombination theory in semiconductors, the nonradiative recombination via defects, typically the Shockley-Read-Hall (SRH) recombination,<sup>[11]</sup> or the tunneling transport especially in GaN-based materials<sup>[12]</sup> plays a dominant role in the low-current regime less than approximately  $1 \mu\text{A}$  (or approximately  $10^{-3} \text{ A cm}^{-2}$ ). Shown in **Figure 2** is an example of the  $I$ - $V$  characteristics expressed as a semi-log plot, measured from a commercial blue LED with a peak wavelength of approximately 450 nm. It is clearly seen that there exist three regions where different mechanisms play the respective dominant roles.

From Figure 2, it is clearly seen that a single exponential function as expressed in Equation (1) is not adequate. To describe the behavior shown in Figure 2 more accurately, two exponential functions of different recombination processes are required here, representing radiative and nonradiative currents in general. Each current has a respective recombination mechanism. Including the ohmic potential drop outside the active region [Equation (2)], one can express the behavior shown in Figure 2 as

$$I = I_r + I_{nr} \cong I_{s,r} e^{q(V-IR_s)/n_r kT} + I_{s,nr} e^{q(V-IR_s)/n_{nr} kT} \quad (3)$$

where  $I_r$  and  $I_{nr}$  represent the radiative and nonradiative currents. The reverse saturation current for each current component is represented by  $I_{s,r}$  and  $I_{s,nr}$  and the ideality factors are included to denote the respective recombination mechanism. For the radiative current, the ideality factor is known to be unity.<sup>[13]</sup> For the non-radiative current involving defects, the ideality factor is

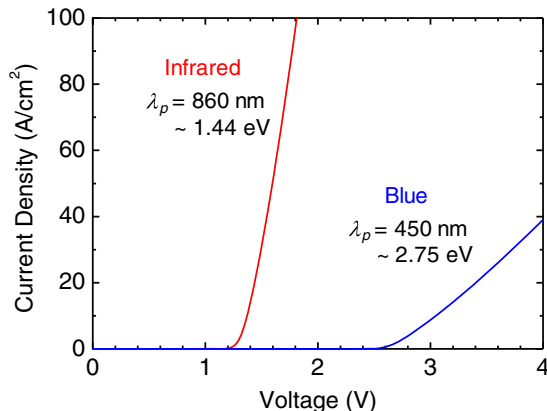


**Figure 1.** Current density as a function of applied voltage for two commercial LED devices with different peak emission wavelengths.

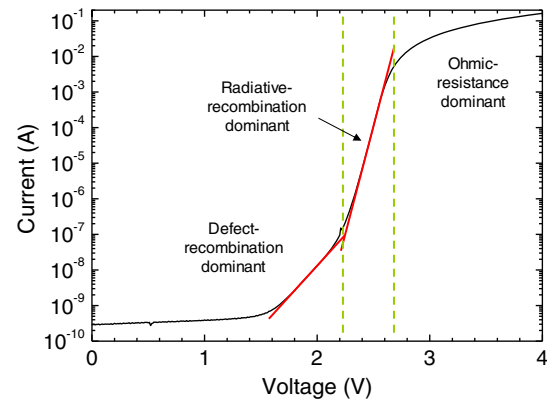


**Figure 2.** Semi-log  $I$ - $V$  curve from a commercial blue LED. Red lines are added to guide the slope change.

two for the SRH recombination and higher for the processes involving tunneling and surface leakage.<sup>[11,14,15]</sup>

The defect current not related with the desired radiative recombination is often called “leakage current,” which is deemed unnecessary and needs to be suppressed as much as possible. The fact that eliminating the leakage current completely is impossible in actuality compels us to devise a useful criterion for judging the amount of leakage current in the LED. One can simplify Equation (3) as a single exponential function with a varying ideality factor  $n_{ideal}$

$$I \cong I_s e^{qV/n_{ideal} kT} \quad (4)$$

The ideality factor is experimentally determined from the measured  $I$ - $V$  curve as follows

$$n_{ideal} = \frac{q}{kT} \left( \frac{\partial \ln I}{\partial V} \right)^{-1} \quad (5)$$

When a varying ideality factor is used, one can track how the dominant recombination mechanism varies depending on the current level. As will be discussed later, one can compare the *minimum* ideality factors to obtain information on the amount of leakage current and the dominance of the desired radiative recombination in LED devices.

## 2.2. S-Parameter

The letter “S” from the S-parameter stands for the “slope” in this case, which is obtained from the plot of  $\log L$  versus  $\log I$ , where  $L$  denotes “light,” or the radiant power (light output power) emitted from the LED device. In the formula, the S-parameter,  $S$ , is defined as<sup>[16]</sup>

$$S = \frac{d \log L}{d \log I} \quad (6)$$

From the recombination theory, the recombination rate  $R$  in the LED can be treated as

$$R = An + Bn^2 + f(n) \quad (7)$$

where  $A$  and  $B$  represent the nonradiative recombination coefficient via the SRH process and the bimolecular recombination coefficient, respectively,  $n$  is the carrier concentration, and  $f(n)$  includes the recombination processes whose power dependence on carrier concentration is other than one or two. The term  $f(n)$  may or may not include the Auger recombination and other nonradiative recombinations at high injection currents, depending on the situation.

Since the radiative recombination rate is proportional to  $n^2$ , the radiant power also has  $n^2$ -dependence. How the charge carriers are consumed under steady state, i.e., whether  $I$  is dominated by  $An$  or  $Bn^2$ , determines the slope of  $\log L$  versus  $\log I$ . In case  $I \sim An$ ,  $L \sim n^2 \sim I^2$ . In assuming  $I \sim R$ , the constant injection efficiency is assumed for simplicity. Thus, when the SRH recombination is dominant at very low injection currents, the S-parameter from  $\log L$  versus  $\log I$  becomes two. **Figure 3** schematically illustrates this case. Similarly, the dominance of the radiative recombination, i.e.,  $I \sim Bn^2$ ,  $L \sim n^2 \sim I$ , leads to the S-parameter of one.

When the injection current further increases, the slope of  $\log L$  versus  $\log I$  becomes smaller than one as the efficiency droop occurs. One can show that the S-parameter is equal to one when the external quantum efficiency (EQE) becomes maximum. Since the EQE,  $\eta_{\text{EQE}}$ , can be written as

$$\eta_{\text{EQE}} = \eta_{\text{LEE}} \frac{I_r}{I} \quad (8)$$

where  $\eta_{\text{LEE}}$  is the light-extraction efficiency (LEE), the EQE maximum requires

$$\frac{d\eta_{\text{EQE}}}{dI} = \eta_{\text{LEE}} \frac{d}{dI} \left( \frac{I_r}{I} \right) = 0 \quad (9)$$

Equation (9) then leads to the condition

$$\frac{dI_r}{dI} I - I_r = 0 \quad (10)$$

which can be rearranged as follows

$$\frac{\frac{1}{I_r} dI_r}{\frac{1}{I} dI} = 1 \quad (11)$$

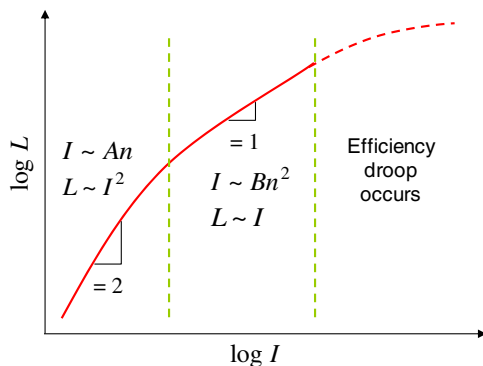


**Figure 3.** Schematic illustration of how the slope changes in  $\log L$  versus  $\log I$  plot. Depending on the power of the carrier concentration in the dominant recombination rate, the slope decreases as the current increases.

Equation (11) can be re-expressed as

$$\frac{d \log I_r}{d \log I} = 1 \quad (12)$$

Since  $L \sim I_r$ , Equation (12) indicates

$$S = \frac{d \log L}{d \log I} = \frac{d \log I_r}{d \log I} = 1 \quad (13)$$

at *maximum* EQEs. From the plot of  $\log L$  versus  $\log I$ , one can get the useful information on the dominance of the radiative recombination over the nonradiative recombination as the injection current increases.

As mentioned earlier, the injection efficiency is assumed to be constant irrespective of the current level when deriving the S-parameter values depending on the recombination mechanism. For more rigorous analysis, including the variable injection efficiency, see Ref. [16]

**Table 1** summarizes the ideality factors and S-parameters for different recombination mechanisms. The two values are actually coincident for each recombination mechanism due to the nature of the carrier concentration being translated into the current and the optical power.

### 2.3. IQE

The IQE is one of the most fundamental performance indicators for LED. The IQE, denoted by  $\eta_{\text{IQE}}$ , is defined as<sup>[17]</sup>

$$\eta_{\text{IQE}} = \frac{\text{number of photons emitted from the active region per second}}{\text{number of electrons injected into the LED per second}} \quad (14)$$

Since the IQE only accounts for the emitted photons from the active region, excluding the LEE, it quantitatively indicates the quality of the epitaxial layers of the LED device. One can measure the IQE by various methods,<sup>[17]</sup> but most widely, either the temperature-dependent electroluminescence (TDEL)<sup>[18]</sup> or the room-temperature reference-point method (RTRM)<sup>[19]</sup> can be used. Since the IQE can be expressed in terms of radiative and nonradiative currents as follows

$$\eta_{\text{IQE}} = \frac{I_r}{I} = \frac{I_r}{I_r + I_{nr}} \quad (15)$$

one can use the information of the IQE to separate the radiative and nonradiative recombination currents from the total injection current.<sup>[20,21]</sup>

When the current starts being injected, the IQE increases from zero as the light is generated, overcoming the nonradiative recombination. It then reaches the maximum and then decreases as the current is further injected into the device. How fast the IQE increases from zero indicates the crystal quality of the epitaxial layers of the sample.

**Table 1.** Ideality factors and S-parameters for different recombination types. for recombination rate  $R \sim n^p$ ,  $n_{\text{ideal}} = 2/p$  and  $S = 2/p$ . A constant injection efficiency is assumed for simplicity.

Recombination type	Ideality factor, S-parameter	Description
Band-to-band radiative	1	Recombination limited by both carriers (electrons and holes)
SRH	2	Recombination limited by a single carrier type (electron or hole, depending on defect types)
Auger	2/3	Three carriers required for recombination
Tunneling	>2	Transport-limited

### 3. Interrelations Between the Minimum Ideality Factor, S-Parameter, and IQE

#### 3.1. Experiments

Two commercial blue LED samples were utilized to demonstrate the interrelations between optoelectronics parameters and show how one can extract information on crystal quality. Both samples were from the same manufacturer and were supposed to have identical epitaxial structures of conventional blue LEDs. The samples, however, had undergone different growth conditions and processing runs, the details of which were not revealed. Both samples had a chip size of  $850 \times 850 \mu\text{m}^2$  and a peak emission wavelength of 445 nm. The samples were mounted on surface-mount-device packages for measurements. For electrical injection, the samples were driven by Keithley 2602 source meter under pulse-current conditions (pulse period: 1 ms, duty cycle: 1%). A Si photodiode was used to detect the emitted light from the device.<sup>[22]</sup>

#### 3.2. Results and Analysis

The measured current density–voltage ( $J$ – $V$ ) curves for the two samples under study (denoted as samples A and B) are shown in **Figure 4**. While sample A shows a higher leakage current than sample B both for the forward and reverse biases, it would be useful to compare the crystal qualities of the samples more quantitatively.

Depicted in **Figure 5** are the ideality factors obtained from the  $J$ – $V$  curves shown in **Figure 4**. Equation (5) has been used after

replacing  $I$  with  $J$ . With the current density increasing from approximately  $10^{-5} \text{ A cm}^{-2}$ , the ideality factor quickly decreases as the radiative recombination rate increases. The ideality factor eventually reaches the minimum as the radiative recombination becomes dominant. After reaching the minimum, the ideality factor increases as the ohmic potential drop outside the active region becomes significant. When comparing the behaviors of the ideality factor for two samples under study, one notices two facts: 1) The ideality factor of sample B approaches the minimum faster than sample A; and 2) the value of the minimum ideality factor is smaller for sample B than for sample A (respective values are 1.45 for sample A and 1.30 for sample B). The first indicates that the radiative recombination in sample B becomes dominant more quickly than in sample A as the injection current increases. The second suggests that the amount of the radiative recombination rate at a given current density is higher in sample B than in sample A. Both reflect that sample B has better crystal quality in the active region than sample A. Although the  $J$ – $V$  curves do not show much difference in the current ranges where the radiative recombination rate becomes dominant, the minimum ideality factor highlights the difference. When compared with the results from other measurements, it becomes more clear that the minimum ideality factor can serve as a useful indicator of the dominant carrier recombination mechanism and crystal quality of the active layer.

**Figure 6** shows the S-parameters obtained from the measured  $L$ – $I$  curves with Equation (6). As the radiative recombination dominates over the nonradiative recombination, the S-parameters quickly approach unity. The value of the S-parameter starts from a number greater than two, indicating that there exist nonradiative

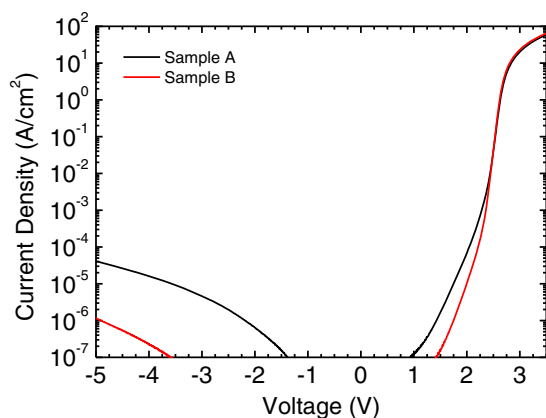


**Figure 4.**  $J$ – $V$  curves of two blue LED samples under study.

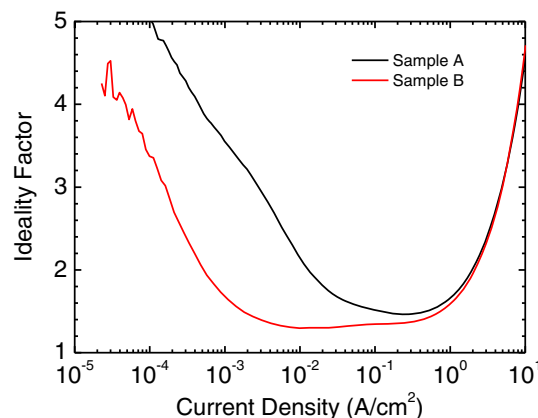


**Figure 5.** Ideality factor obtained from the  $J$ – $V$  curves for two blue LED samples under study.

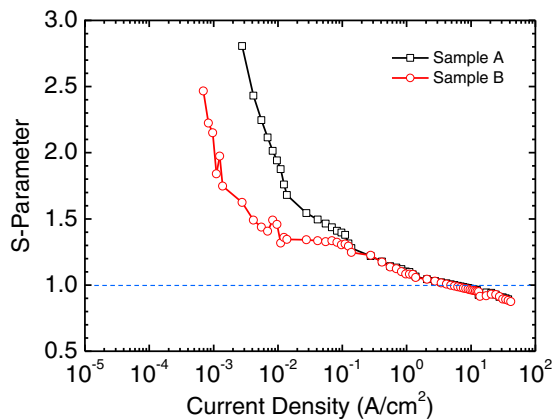


**Figure 6.** S-parameters obtained from the two blue LED samples under study.

recombination mechanisms other than the SRH process, involving such processes as tunneling via defects and/or recombination on etched mesa surfaces, in very low current ranges. The fact that the S-parameter of sample B approaches unity faster than sample A indicates the difference in defect level between the two samples. As observed from the ideality factors shown in Figure 5, the S-parameter also accurately depicts how the radiative recombination becomes dominant over the nonradiative recombination as the injection current increases. While the ideality factor increases after reaching the minimum with increasing current, the S-parameter keeps decreasing below unity as the efficiency droop occurs.

**Figure 7** demonstrates the IQEs measured by the RTRM for samples under study. Both IQEs increase rapidly from zero as the radiative recombination becomes dominant with the injection-current increase. As indicated by the ideality factors

and the S-parameters, the IQE for sample B increases from zero at a lower current density and stays higher until it reaches the maximum. Also, the value of the maximum IQE for sample B is observed to be higher than that for sample A. The IQE behaviors just described are all consistent with the observations on the ideality factors and S-parameters. It has been observed from various experiments on LEDs that the maximum IQE values closely correlate with minimum ideality factors: when the minimum ideality factor is small, the maximum IQE value is large.<sup>[23–25]</sup> The observed correlation between the minimum ideality factor and the maximum IQE value has not been explicitly pointed out and its significance has not yet been recognized as such. Therefore, in this work, we propose that the minimum ideality factor can serve as a useful guide reflecting the crystal quality of the epitaxial layers of the LED device.

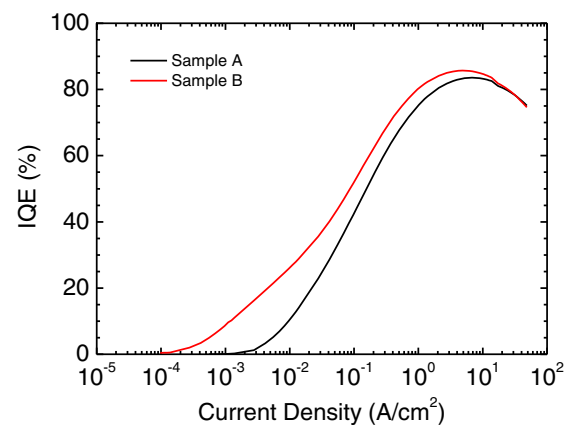


**Figure 7.** IQE data obtained by the RTRM for two blue LED samples under study.

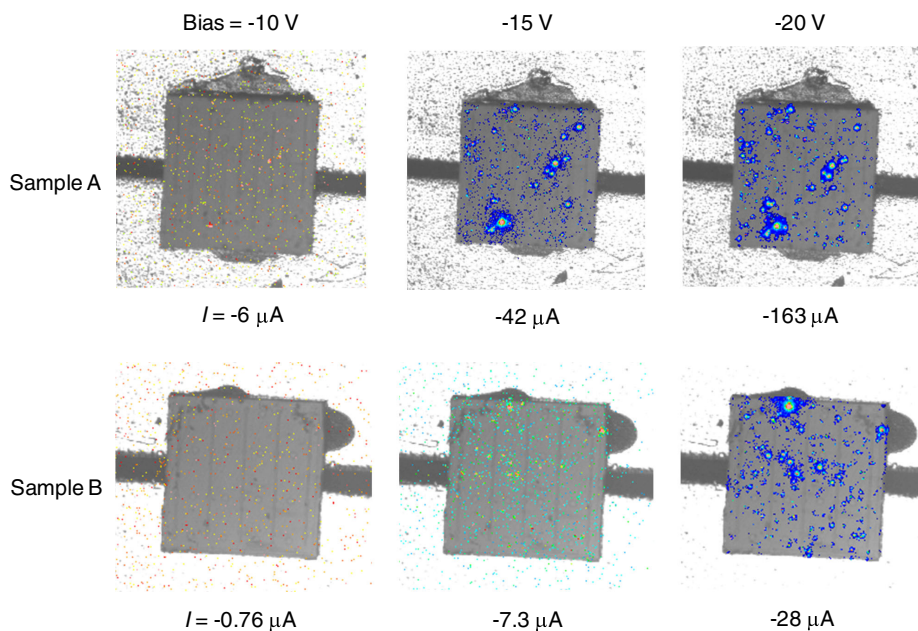


**Figure 8.** Localized emissions from samples A and B under various reverse-bias voltages, measured by a high-resolution emission microscope.



**Table 2.** Various macroscopic measurement parameters from  $I$ - $V$  and  $L$ - $I$  data for two samples under study. The smaller minimum ideality factor is correlated with the higher maximum IQE. The current density value at the maximum IQE closely follows the current density at  $S = 1$ .

Sample	Minimum Ideality Factor	Maximum IQE [%]	Current Density at Max IQE [ $\text{A cm}^{-2}$ ]	Current Density at $S = 1$ [ $\text{A cm}^{-2}$ ]
Sample A	1.45	83.6	6.92	5.54
Sample B	1.30	85.7	4.84	4.84

Show in **Figure 8** are the localized dot-like emissions from the samples under study at various reverse-bias voltages, measured by a high-resolution emission microscope (Hamamatsu PHAMOS-1000). It is clearly seen that sample A with a higher minimum ideality factor shows more dot-like emissions, indicating more defects, especially threading dislocations, in the crystals.<sup>[26]</sup>

**Table 2** summarizes the minimum ideality factor and the maximum IQE values for samples A and B. Sample B, which has a smaller minimum ideality factor of 1.30, has a higher maximum IQE value of 85.7% while sample A has a minimum ideality factor of 1.45 and a maximum IQE of 83.6%. The current density at the maximum IQE also correlates with the current density at which  $S = 1$  although there exists a slight discrepancy, especially with Sample A, possibly caused by the measurement errors.

## 4. Conclusion

We have examined the macroscopic measurements such as  $I$ - $V$  and  $L$ - $I$  and demonstrated how one can extract information on the defect level from the parameters from those macroscopic measurements. Especially, the ideality factor and the  $S$ -parameter have been shown to contain useful information on the defect level and the crystal quality of the active region in the LED devices. From how fast the ideality factor and the  $S$ -parameters decreases with increasing current, one can obtain information on how the radiative recombination dominates over the nonradiative recombination. The value of the minimum ideality factor can be utilized to indicate the crystal quality of the epitaxial layers: the smaller the minimum ideality factor, the better the epitaxial crystal quality of the device. Since the defect level and crystallinity of the materials used for the light-emitting devices are critically important, a useful figure of merit such as the minimum ideality factor suggested here can be employed for characterization of devices fabricated from various epitaxially grown materials with different device structures.

## Acknowledgements

This work was supported by the Technology Innovation Program funded by the Ministry of Trade, Industry and Energy, Republic of Korea, under Grant 20006908.

## Conflict of Interest

The authors declare no conflict of interest.

## Data Availability Statement

The data that support the findings of this study are available from the corresponding author upon reasonable request.

## Keywords

characterization, defects, ideality factor, internal quantum efficiency, light-emitting diodes,  $S$ -parameter

Received: January 19, 2022  
Published online: February 20, 2022

- [1] M. A. Reshchikov, H. Morkç, *J. Appl. Phys.* **2005**, 97, 061301.
- [2] X. A. Cao, K. Topol, F. Shahedipour-Sandvik, J. Teetsov, P. M. Sandvik, S. F. LeBoeuf, A. Ebong, J. Kretschmer, E. B. Stokes, S. Arthur, A. E. Kaloyeros, D. Walker, *Proc. SPIE* **2002**, 4776, 105.
- [3] S. J. Ronser, E. C. Carr, M. J. Luydowise, G. Girolami, H. I. Erikson, *Appl. Phys. Lett.* **1997**, 70, 420.
- [4] A. Uddin, A. C. Wei, T. G. Andersson, *Thin Solid Films* **2005**, 483, 378.
- [5] X. A. Cao, P. M. Sandvik, S. F. LeBoeuf, S. D. Arthur, *Microelectron. Reliab.* **2003**, 43, 1987.
- [6] F. A. Ponce, D. Cherns, W. T. Young, J. W. Steeds, *Appl. Phys. Lett.* **1996**, 69, 770.
- [7] A. Sakai, *Appl. Phys. Lett.* **1998**, 73, 481.
- [8] A. N. Bright, N. Sharma, C. J. Humphreys, *J. Electron Microsc.* **2001**, 50, 489.
- [9] Z. Liliental-Weber, *Jpn. J. Appl. Phys.* **2014**, 53, 100205.
- [10] P. J. Hansen, Y. E. Strausser, A. N. Erickson, E. J. Tarsa, P. Kozodoy, E. G. Brazel, J. P. Ibbetson, U. Mishra, V. Narayanamurti, S. P. DenBaars, J. S. Speck, *Appl. Phys. Lett.* **1998**, 72, 2247.
- [11] D. Neamen, *An Introduction to Semiconductor Devices*, McGraw-Hill, New York, NY **2005**.
- [12] N. I. Bochkareva, V. V. Voronenkov, R. I. Gorbunov, A. S. Zubrilov, Y. S. Lelikov, P. E. Latyshev, Y. T. Rebane, A. I. Tsyuk, Y. G. Shreter, *Appl. Phys. Lett.* **2010**, 96, 133502.
- [13] G. W. Lee, J.-I. Shim, D.-S. Shin, *Appl. Phys. Lett.* **2016**, 109, 031104.
- [14] X. A. Cao, E. B. Stokes, P. M. Sandvik, S. F. LeBoeuf, J. Kretschmer, D. Walker, *IEEE Electron Dev. Lett.* **2002**, 23, 535.
- [15] D. Zhu, J. Xu, A. N. Noemaun, J. K. Kim, E. F. Schubert, M. H. Crawford, D. D. Koleske, *Appl. Phys. Lett.* **2009**, 94, 081113.
- [16] K.-S. Kim, D.-P. Han, H.-S. Kim, J.-I. Shim, *Appl. Phys. Lett.* **2014**, 104, 091110.
- [17] J.-I. Shim, D.-S. Shin, *Nanophotonics* **2018**, 7, 1601.
- [18] D.-S. Shin, D.-P. Han, J.-Y. Oh, J.-I. Shim, *Appl. Phys. Lett.* **2012**, 100, 153506.
- [19] J.-I. Shim, D.-P. Han, C.-H. Oh, H. Jung, D.-S. Shin, *IEEE J. Quantum Electron.* **2018**, 54, 8000106.
- [20] I.-G. Choi, D.-P. Han, J. Yun, K. S. Kim, D.-S. Shin, J.-I. Shim, *Appl. Phys. Express* **2013**, 6, 052105.
- [21] C.-H. Oh, D.-S. Shin, J.-I. Shim, *IEEE Photon. Technol. Lett.* **2019**, 31, 1441.
- [22] C.-H. Oh, J.-I. Shim, D.-S. Shin, *Jpn. J. Appl. Phys.* **2019**, 58, SCCC08.
- [23] A. B. M. H. Islam, J.-I. Shim, D.-S. Shin, *Materials* **2018**, 11, 743.
- [24] A. B. M. H. Islam, D.-S. Shin, J.-I. Shim, *Appl. Sci.* **2019**, 9, 871.
- [25] A. B. M. H. Islam, J.-I. Shim, D.-S. Shin, *Phys. Status Solidi A* **2022**, 219, 2100418.
- [26] M. Meneghini, S. Vaccari, N. Trivellin, D. Zhu, C. Humphreys, R. Butendheich, C. Leirer, B. Hahn, G. Meneghesso, E. Zanoni, *IEEE Trans. Electron. Dev.* **2012**, 59, 1416.